Reduction of Horse Heart Ferricytochrome *c* by Bovine Liver Ferrocytochrome b_5. Experimental and Theoretical Analysis†

Lindsay D. Eltis,‡ Robert G. Herbert,§ Paul D. Barker,‡ A. Grant Mauk,*,‡ and Scott H. Northrup*,§

Department of Biochemistry, University of British Columbia, Vancouver, British Columbia V6T 1W5, Canada, and Department of Chemistry, Tennessee Technological University, Box 5055, Cookeville, Tennessee 38505

Received May 21, 1990; Revised Manuscript Received January 2, 1991

ABSTRACT: The reduction of horse heart ferricytochrome *c* by the tryptic fragment of bovine liver cytochrome b_5 and its dimethyl ester heme (DME)-substituted derivative has been studied as a function of ionic strength, pH, and temperature under solution conditions where the reaction is bimolecular. The rate constant for ferricytochrome *c* reduction by native ferrocytochrome b_5 is 1.8 (±0.2) × 10^7 M^{-1} s^{-1} (25 °C) with $\Delta H^{\ddagger}$ = 7.5 (±0.2) kcal/mol and $\Delta S^{\ddagger}$ = −0.3 (±0.6) eu (pH 7.0, I = 0.348 M). Under the same solution conditions, the reduction of ferricytochrome *c* by DME-ferrocytochrome b_5 proceeds with a rate constant of 1.7 (±0.1) × 10^7 M^{-1} s^{-1} with $\Delta H^{\ddagger}$ = 7.9 (±0.4) kcal/mol and $\Delta S^{\ddagger}$ = 1 (±1) eu. The rate constants for both reactions are strongly dependent on ionic strength. A detailed electrostatic analysis of the proteins has been performed. Two relatively simple Brownian dynamics simulation models predict rate constants for the reaction between the two native proteins that demonstrate a dependence on ionic strength similar to that observed experimentally. In one of these models, the proteins are treated as spheres with reactive surface patches that are defined by a 5° cone generated about the dipole vector calculated for each protein and aligned with the presumed electron-transfer site near the partially exposed heme edge. The second model replaces the reactive patch assumption with an exponential distance dependence for the probability of reaction that permits estimation of a value for the distance-dependence factor α. Calculations with this latter model in combination with the aligned dipole assumption provide a reasonable approximation to the obseved ionic strength dependence for the reaction and are consistent with a value of α = 1.2 $Å^{-1}$.

Identification and quantification of the factors that determine the rate of electron transfer between metalloproteins are fundamental to development of an understanding of the regulatory mechanisms that have evolved to control such reactions in vivo. Consequently, experimental and theoretical analysis of the reactions between metalloproteins of known three-dimensional structure has been a topic of considerable recent activity (e.g., Marcus & Sutin, 1985; King et al., 1985; Gray, 1986; Northrup et al., 1986b, 1988; Mayo et al., 1986; Hoffman & Ratner, 1987; Hazzard et al., 1987; Summers & Erman, 1988; Wendoloski et al., 1987; Dixon et al., 1989, 1990). Of the protein–protein electron-transfer reactions that are suitable for such studies, the reduction of ferricytochrome *c* by ferrocytochrome b_5 is particularly attractive because both proteins are relatively small (MW = 10000–12500), undergo minimal oxidation state dependent structural change (Argos & Mathews, 1975; Takano & Dickerson, 1980, 1981), and are readily modified by site-directed mutagenesis (Pielak et al., 1985; von Bodman et al., 1986; Funk et al., 1990). Previous experimental studies of electron transfer between these two proteins have been of two principal types. First, the steady-state studies of Millett and co-workers (Ng et al., 1977; Stonehuerner et al., 1979) have considered the reaction between specifically modified forms of cytochrome *c* and native cytochrome b_5 to evaluate the involvement of specific cytochrome *c* lysyl residues proposed by Salemme (1976) to be critical to formation of a cytochrome b_5–cytochrome *c* electron-transfer complex. The second type of study has emphasized the consideration of intramolecular electron transfer (McLendon et al., 1985; McLendon & Miller, 1985). These studies have involved two strategies: (a) mixing native cytochrome b_5 with a photosensitive derivative of cytochrome *c* at low ionic strength and monitoring photoinduced electron transfer from the modified cytochrome *c* to cytochrome b_5 or (b) performing a similar experiment in which intramolecular electron transfer is initiated by pulse radiolysis (McLendon & Miller, 1985). Studies of this type in which various heme-modified or heme-substituted forms of cytochrome *c* or cytochrome b_5 are employed have been used to assess the influence of thermodynamic driving force on the observed rates (McLendon & Miller, 1985). Previous theoretical analyses of the reaction between these two proteins have been restricted to interactive molecular graphics docking (Salemme, 1976) augmented by electrostatics (Mauk et al., 1986) or molecular dynamics calculations (Wendoloski et al., 1987).

Interestingly, little experimental (Strittmatter, 1964) or theoretical (Marcus & Sutin, 1985) treatment is available concerning the kinetics of ferricytochrome *c* reduction by ferrocytochrome b_5 under solution conditions where the reaction is bimolecular and both proteins have been purified to homogeneity. We have now studied this reaction and the reduction of ferricytochrome *c* by dimethyl ester heme substituted cytochrome b_5 as a function of pH, temperature, and ionic strength to gain greater insight into the structural and functional properties of these two cytochromes that dictate the rate of electron transfer between them under conditions where the reaction is second order. To assist in interpretation of these results, modeling calculations that employ a variety of simplifying assumptions have been undertaken in an attempt to rationalize the experimentally observed ionic strength, temperature, and pH dependences of these rate constants. The

† This work was supported by NIH Grants DK01403 (S.H.N.), GM34248 (S.H.N.), and GM33804 (A.G.M.), and acknowledgment is made to the donors of the Petroleum Research Fund, administered by the American Chemical Society, for support of this work (S.H.N.). L.D.E. was supported by a Medical Research Council studentship, P.D.B. is the recipient of an I. W. Killam postdoctoral fellowship, and S.H.N. is a recipient of an NIH Research Career Development Award.

‡ University of British Columbia.

§ Tennessee Technological University.

0006-2960/91/0430-3663$02.50/0

Brownian dynamics (BD) computer simulation method (Northrup et al., 1984, 1986a; Allison et al., 1985) employed here for this purpose has been recently used in a number of applications to compute bimolecular diffusion-controlled rate constants between species interacting through complicated potential fields and highly asymmetric reaction criteria. In this approach, the Brownian motion of interacting macromolecules is simulated stochastically by a series of small displacements chosen from a distribution which is equivalent to the short-time solution of the Smoluchowski diffusion equation. Reaction probabilities generated in this fashion are converted exactly to bimolecular rate constants by a formula connecting diffusive fluxes to probabilities. This approach has been applied successfully to calculate the electrostatic influences in reactions of superoxide dismutase enzyme with superoxide anion (Sharp et al., 1987a,b), carbonic anhydrase enzyme–substrate reactions (Reynolds et al., 1990), electron transfer between cytochrome *c* and cytochrome *c* peroxidase (Northrup et al., 1986b, 1987a,b, 1988), and electron self-exchange in cytochrome c_{551} (Northrup & Herbert, 1989). This theory provides an interpretative framework for understanding the role of electrostatic influences, ionic strength, temperature, and pH effects, and geometric reactive criteria in the bimolecular rates observed in the experiments.

Experimental Methods

General Methods. Glass-distilled water purified with a Barnstead NANOpure system to a resistivity of 16–17 MΩ was used in preparation of all solutions. Measurements of pH were performed with a Radiometer Model PHM 84 meter fitted with a Radiometer type GK 2321C combination electrode. Phosphate buffers of desired pH and ionic strength were prepared from monobasic and dibasic sodium salts (BDH). Lumiflavin was obtained from Sigma.

Protein Purification. The tryptic fragment of bovine hepatic cytochrome b_5 and its dimethyl ester heme substituted derivative were prepared as described previously (Reid & Mauk, 1982; Reid et al., 1984). Horse heart cytochrome *c* (type VI) was purchased from Sigma Chemical Co. and purified by anion-exchange chromatography to remove deamidated cytochrome (Brautigan et al., 1978). Protein solutions were concentrated by ultrafiltration using Amicon-52 stirred cells fitted with YM-5 membranes or by centrifugal ultrafiltration using Centripreps and Centricons (Amicon). Protein concentrations were determined with values of $\epsilon_{409.5} = 106.1\ mM^{-1}$ (Margoliash & Frohwirt, 1959) and $\epsilon_{412.5} = 117.0\ mM^{-1}$ (Ozols & Strittmatter, 1964) for ferricytochromes *c* and b_5, respectively.

Kinetic Measurements and Data Analysis. Rapid-mixing experiments were performed with a Dionex Model D-103 stopped-flow spectrophotometer (2-cm observation path length) that was interfaced to a Zenith Model Z-100 microcomputer by On-Line-Instrument-Systems (Jefferson, GA). The transfer of reactants into the drive syringes of the stopped-flow spectrophotometer and the drive syringe plungers involved modifications to this system that have been described previously (Reid & Mauk, 1982; Scott, 1979). The sensitivity of ferrocytochrome b_5 to autoxidation in the absence of excess reductant (Berman et al., 1976) necessitated the installation of the stopped-flow apparatus into an argon-filled glovebox (Vacuum/Atmospheres Model HE-243-2 with Model HE-493 Dri-Train) in an arrangement modeled on that of Leung et al. (1989) as described in detail elsewhere (Eltis, 1989).

Reduction of ferricytochrome *c* by ferrocytochrome b_5 was studied under second-order conditions with the reactants at equimolar concentrations (~1.7 μM). Ferricytochrome *c* was prepared by the addition of an excess of ammonium bis(dipicolinato)cobaltate(III) (Mauk et al., 1979). Excess oxidant was removed from the cytochrome by passing the sample over a 10 × 0.5 cm column of Sephadex G-25 superfine resin. The solutions were placed in glass serum bottles that were sealed with cleaned serum stoppers. These solutions were then purged for 30 min with prepurified argon that had been passed through a 20-cm column of Chemalog Catalyst R3-11 and humidified by passage through water. After 30 min, 0.2 equiv of lumiflavin (40 μL) was introduced into the cytochrome b_5 solution with a gas-tight syringe, and ferricytochrome b_5 was reduced by illumination of this solution for 30 min. The puncture holes in the serum stoppers were sealed with electrical tape, and the serum bottles were transferred into the glovebox.

Oxidation of ferrocytochrome b_5 was monitored at 428 nm, where the total absorbance and the change in absorbance of cytochrome *c* are small. The reduction of ferricytochrome *c* was monitored at 416 nm, an isosbestic point in the electronic absorption spectra of ferri- and ferrocytochrome b_5. At least five decay curves were averaged at each wavelength, and the data were fitted to a second-order rate expression using the nonlinear least-squares fitting program MINSQ (MicroMath Scientific Software). At lower values of ionic strength, the initial portion of the reaction occurred within the dead time of the instrument. In these cases, the initial concentration of the cytochromes was determined by normalizing the overall change of absorbance to the total change in absorbance observed for the reaction performed at high ionic strength. The second-order rate constants obtained by this method were compared with rate constants obtained by two alternative methods in the following control experiments. First, the reactions were performed under pseudo-first-order conditions with ferricytochrome *c* in 5–30-fold molar excess over ferrocytochrome b_5 (1 μM). A greater excess of cytochrome *c* could not be used in these measurements owing to the high background absorbance inherent at such high cytochrome concentrations and to the limited time resolution of the stopped-flow technique. Second, the possible influence of lumiflavin on the observed second-order rate constant was evaluated in control measurements in which ferrocytochrome b_5 was produced by anaerobic reduction of the protein by sodium dithionite. In this experiment, several grains of fresh dithionite were added to a sample of ferricytochrome b_5 under argon, the excess reductant was removed by eluting the solution over a small column of Sephadex G-25 prepared in the glovebox, and the rate of ferricytochrome *c* reduction was monitored under second-order conditions.

The dependence of the second-order rate constants for ferricytochrome *c* reduction by ferrocytochrome b_5 on ionic strength was initially analyzed in terms of the van Leeuwen (1983) relationship as defined by

$$\ln k = \ln k_\infty - [Z_1Z_2 + ZP(1 + \kappa R) + PP(1 + \kappa R)^2]\left[\frac{q^2}{4\pi\epsilon_0\epsilon k_B TR}\right] f(\kappa) \quad (1a)$$

where

$$ZP = \frac{Z_1P_2 + Z_2P_1}{qR} \quad (1b)$$

$$f(\kappa) = \frac{1 - e^{-2\kappa R_2}}{2\kappa R_2(1 + \kappa R_1)} \quad (1c)$$

and where $R = R_1 + R_2$, $PP = P_1P_2/(qR)^2$, $\kappa = 0.329I^{1/2}$, Z_1

Table I: Electrostatic Properties of Cytochrome c, Cytochrome b_5, and DME-Cytochrome b_5 as a Function of Ionic Strength (pH 7.0)[a]

	cytochrome c				cytochrome b_5				DME-cytochrome b_5			
I (M)	q	q_d	d	γ	q	q_d	d	γ	q	q_d	d	γ
0.094	7.13	±1.96	283.9	30.49	−9.06	±4.61	637.8	142.17	−6.82	±3.73	516.6	130.04
0.190	7.18	±1.96	284.1	30.14	−9.15	±4.62	638.8	142.13	−6.93	±3.75	518.9	130.22
0.286	7.21	±1.96	284.1	29.97	−9.19	±4.62	639.4	142.11	−6.98	±3.76	520.0	130.30
0.482	7.24	±1.96	284.1	29.73	−9.24	±4.63	639.8	142.08	−7.04	±3.77	521.1	130.37
0.977	7.27	±1.96	284.0	29.49	−9.29	±4.63	640.1	142.03	−7.10	±3.77	522.0	130.41

[a] q = net protein monopole (units of electron charge); q_d = dipole charge (units of electron charge); d = dipole magnitude (debye); γ = angle between dipole and Fe vector.

Table II: Electrostatic Properties of Cytochrome c, Cytochrome b_5, and DME-Cytochrome b_5 as a Function of pH (I = 0.482 M)[a]

	cytochrome c				cytochrome b_5				DME-cytochrome b_5			
pH	q	q_d	d	γ	q	q_d	d	γ	q	q_d	d	γ
6.0	8.40	±1.79	259.4	20.71	−7.35	±4.96	685.9	145.44	−4.66	±3.92	542.1	133.48
6.5	7.70	±1.89	274.2	25.97	−8.35	±4.80	663.3	143.62	−5.92	±3.85	532.9	131.77
7.0	7.24	±1.96	284.1	29.74	−9.24	±4.63	639.8	142.08	−7.04	±3.77	521.1	130.37
7.5	6.93	±1.98	286.4	31.50	−9.92	±4.47	618.2	141.35	−7.85	±3.65	505.2	129.62
8.0	6.54	±1.94	281.1	32.59	−10.50	±4.28	592.0	141.20	−8.48	±3.48	480.8	129.11

[a] q = net protein monopole (units of electron charge); q_d = dipole charge (units of electron charge); d = dipole magnitude (debye); γ = angle between dipole and Fe vector.

and Z_2 are the monopole charges on ferricytochrome c and ferrocytochrome b_5, R_1 and R_2 are the radii of the two proteins, q is the elementary charge, ϵ_0 is the dielectric permittivity, ϵ is the dielectric constant of water, k_B is Boltzmann's constant, and P_1 and P_2 are the components of the dipoles of the proteins through their respective exposed heme edges. For cytochrome b_5, the heme edge was taken to be the γ-methine carbon, and in cytochrome c, the heme edge was taken to be the methyl carbon of the most solvent-exposed heme pyrrole.

Theoretical Methods

Electrostatic Properties of the Proteins. The electrostatic properties of horse heart ferricytochrome c (Bushnell et al., 1990) and trypsin-solubilized bovine liver ferrocytochrome b_5 (Argos & Mathews, 1975; Bernstein et al., 1977) were calculated from X-ray crystallographic coordinates obtained from the sources indicated. The net protein charge and dipole orientation and magnitude for both proteins were computed by assigning partial charges to each atom in the protein according to standard partial charge values (Northrup et al., 1981). For the pH range from 6 to 8, all lysyl and arginyl residues were assumed to be fully protonated, and the aspartyl, glutamyl, carboxyl-terminal, and heme propionate groups were assumed to be dissociated (Matthew, 1985). The charge status of the α-amino group and of histidyl residues was estimated by application of static-accessibility-modified Tanford–Kirkwood calculations (Tanford & Kirkwood, 1957; Tanford & Roxby, 1972; Shire et al., 1974) at all values of pH and ionic strength studied using a program provided by Dr. James B. Matthew. Horse heart ferricytochrome c has an uncharged, acetylated amino terminus. Unlike previous BD studies, the hydrogen atoms were modeled onto the peptide nitrogens to generate the additional N–H dipolar pair on each residue. However, this effect was found to be negligible. Tables I and II show the net monopole and dipole moments of the proteins produced by these calculations as a function of ionic strength and pH, respectively. The dipole moments of the proteins are computed by the equations provided by Koppenol and Margoliash (1982) for macromolecules with net charge.

Simplified Dipolar Sphere Models for Brownian Calculations. For purposes of computational facility in initial BD simulation studies of association rates, a simplified model (Northrup, 1986b) of the two proteins based on the electrostatic results outlined above has been employed. Simple models are useful in that they can more quickly generate rate constants over a wide range of parameters and environmental conditions than more rigorous simulations and give one important qualitative insight. We have modeled both proteins as charged spheres having a centrally imbedded monopolar charge carrying the net protein charge and two dipolar charges imbedded 1.5 Å inside the protein surface, with magnitudes computed to generate the dipole moments calculated above. As the proteins are actually somewhat elliptical in shape rather than spherical, the estimation of effective radius has a degree of arbitrariness. Table III summarizes the dipolar sphere model parameters for each protein in the two different models.

Table III: Parameters for the Monopole–Dipole Spheres Model of the Cytochrome c–Cytochrome b_5 Reaction

parameter	cytochrome c	cytochrome b_5	DME-cytochrome b_5
R_i, protein hard-sphere radius (Å)	16.6	15.9	15.9
$D_{tr,i}$ (cm^2/s)	1.47×10^{-6}	1.54×10^{-6}	1.54×10^{-6}
$D_{rot,i}$ (s^{-1})	4.01×10^{7}	4.57×10^{7}	4.57×10^{7}
Fe distance from center-of-mass (Å)	5.26	10.3	10.3
dipole charges distance from center-of-mass (Å)	15.1	14.4	14.4

The translational diffusion coefficients were estimated by the Stokes–Einstein relationship $D_{tr,i} = k_BT/6\pi\eta R_i$ with stick boundary conditions, where k_BT is the product of Boltzmann's constant and absolute temperature. Values in Table III are for aqueous solution at 25 °C with a viscosity of η = 0.89 cP. Rotational and translational diffusion are assumed to be hydrodynamically uncoupled for this simulation. Rotational diffusion constants for each protein are estimated by using the equation for spherical particles, $D_{rot,i} = k_BT/8\pi\eta R_i^3$, to produce the numerical values shown in Table III. Two models have been explored for the orientation dependence of reactivity as described separately below (see Reaction Criteria).

The electrostatic field effects in the diffusional association rate are treated here in an approximate fashion for computational facility. The electrostatic field is generated by assigning three charges to each protein: a monopole and two dipole charges. Monopole charges are placed at the centers of the spheres and carry the net protein charge. Dipole charges are placed at opposite ends of the computed dipole axis at 1.5

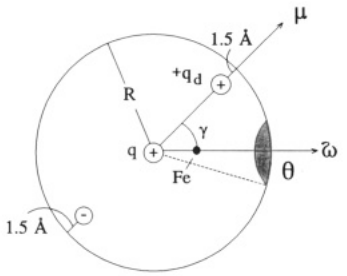

FIGURE 1: Schematic representation of the dipolar sphere model used to simplify the BD simulation of the reaction between ferrocytochrome b_5 and ferricytochrome c. Values for the various quantities shown here are given in Table I.

Å inside the surface of the proteins. This placement prohibits singularities in the electrostatic potential when proteins collide along dipole vectors. Dipole charge magnitudes necessary to generate the appropriate dipole strength are listed in Tables I and II. The choice of surface charges rather than a centrally located point dipole of the same magnitude is made (a) to reflect qualitatively the presence of most charged groups near the surface of the protein and (b) to correspond to the recent finding by Northrup et al. (1987a,b, 1988) that the local charge density near the reactive site is more significant in diffusional reaction dynamics of dipoles than are global electrostatic features.

The solvent water is treated as a dielectric continuum with a dielectric constant $\epsilon = 78.7$ (25 °C) in the following simulations. For the purposes of these simplified model studies, it would be superfluous as well as computationally expensive to attempt to incorporate the discontinuity in the dielectric constant across the protein–solvent interface, although for future studies it will be critical to use more accurate treatments of electrostatic fields around charged macromolecules in water (Harvey, 1989). We include ionic strength effects using a Debye–Hückel screening term in the electrostatic potential energy equation:

$$U = \sum\sum(q_i q_j/\epsilon r_{ij}) \exp[-\kappa(r_{ij} - B_{ij})]/(1 + \kappa B_{ij}) \quad (2)$$

where summations i and j are over charges on proteins 1 and 2, q_i is the electrostatic charge i, r_{ij} is the separation distance between charges i and j, $\kappa = 0.327I^{1/2}$ is the Debye–Hückel screening parameter in units Å^{-1}, I is ionic strength, and B_{ij} is a distance shifting factor for charge i, j interaction included to account approximately for the finite size of ions. The finite ion size correction B_{ij} has been found to be extremely important in simulations involving large molecules (Northrup et al., 1986b) and is given by the empirical term $B_{ij} = b_i + b_j$, where b_i is the distance that charge i is imbedded inside the spherical protein surface.

Reaction Criteria. Simulations were performed in which two different descriptions of the electron-transfer reaction were employed. In the Patch model, each protein is assumed to be anisotropically reactive and to possess a reactive zone of angles extent θ_{cytc},θ_{cytb5} that is axially symmetric around an orientation vector ω as shown in Figure 1. The vector ω is assumed to pass through the iron atom. Reaction is defined as occurring instantaneously when protein separation equals collisional separation ($R = R_{cytc} + R_{cytb5}$) and the interprotein separation vector passes through both reactive zones. This model system is the same as that employed in previous BD simulations by Northrup et al. (1986b) and as the classic model of Solc and Stockmayer (1973). The angle size of the electron-transfer surface on cytochromes is an unknown quantity and is left here as an adjustable parameter. Values for this parameter can be obtained on the basis of estimates of fractional surface area of heme exposure. This approach renders angle values of 5° and 12° for cytochrome c and cytochrome b_5, respectively, when heme exposure area percentages of 0.19 and 1.11 provided by Dixon et al. (1989) are employed. However, as collision of the heme edges may not be necessary for electron transfer to occur, these values may not have great meaning in this context.

An exponential model of the electron-transfer event (Northrup & Herbert, 1989) has also been studied. In this case, we define an intrinsic spatially dependent electron-transfer rate constant $k_{et}(r_{FeFe})$ given by

$$k_{et}(r_{FeFe}) = k_{et}(r_0) \exp[-\alpha(r_{FeFe} - r_0)] \quad (3)$$

Here, $k_{et}(r_0)$ is the electron-transfer rate constant when porphyrins are in direct contact edge-on and is assumed (Guarr et al., 1983) to be 10^{11} s^{-1} for our study. The Fe–Fe distance in such an arrangement is determined to be $r_0 = 11.7$ Å by molecular graphics docking experiments on two free porphyrins. Even faster electron-transfer rates would occur for porphyrins in a sandwich orientation at contact (Siders et al., 1984), but such orientations are not considered because the heme groups are perpendicular to the protein surface. The electron-transfer distance-dependent factor α is a quantity of intense interest (Mayo et al., 1986; McLendon, 1988) and is an adjustable parameter of our study which can be varied to fit the experimental data. Thus, an estimate of this important factor can be obtained from BD.

When the above intrinsic reactivity function is used, the spatially dependent probability P that the reactant pair survives a given Brownian step of duration δt without electron transfer is then $P = \exp(k_{et}\delta t)$. This probability is multiplicative throughout the trajectory, and the final value gives the escape probability for that trajectory. The exponential represented in eq 3 has the flavor of the Siders et al. (1985) theory for orientation and distance dependence of electron transfer between porphyrins.

Brownian Dynamics Simulations. The basic BD trajectory simulation method (Northrup et al., 1984) and its extensions (Allison et al., 1985; Northrup et al., 1986a) have been previously described. The trajectory of a reactive pair undergoing translational and rotational diffusion in a viscous medium is simulated stochastically by a series of small random displacements chosen from a distribution which is the short-time solution of the Smoluchowski diffusion equation. Northrup et al. (1986a) have incorporated accurate algorithms of Lamm and Schulten (1983) for particle displacements near absorbing and reflecting boundaries, thereby allowing larger time steps to be chosen than are permitted by use of the free diffusion algorithm of Ermak and McCammon (1978) near a boundary. As both particles are macromolecules and are of comparable size, the rotational relaxation times of the two are comparable and on the time scale of translational diffusional relaxation, so rotational dynamics is expected to contribute strongly to the resulting rate calculation. More quantitatively accurate results should be obtained in future studies that include the hydrodynamic coupling between rotational and translational diffusion (Dickinson, 1985). By simulation of a large number of trajectories (50 000 for each of the cases studied), we calculated the probability $p(b)$ for the reactive encounter of a particle pair starting their diffusion at randomly selected orientations a fixed separation distance $b = 72.5$ Å outside the region of forces. Truncation of unsuccessful trajectories is performed at separation surface $c = 200$ Å, and an exact truncation correction is applied as described by Northrup et

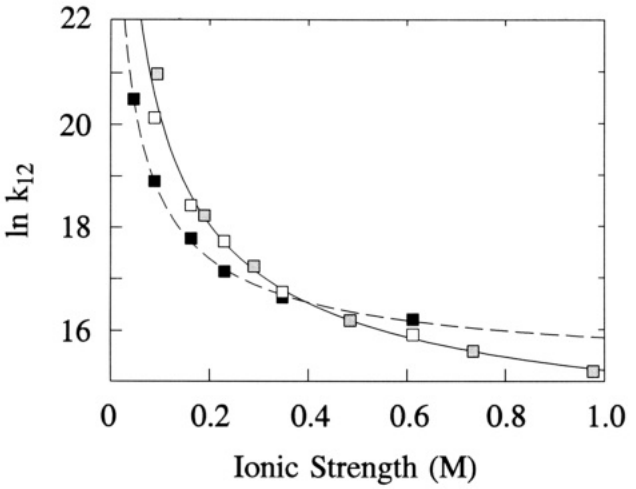

FIGURE 2: Ionic strength dependence of the bimolecular rate constant of the reduction of ferricytochrome c by native and DME-ferrocytochrome b_5 (pH 7.0, 25.0 °C): (□) reaction between native ferrocytochrome b_5 and ferricytochrome c with sodium phosphate as the only electrolyte present; (stippled squares) same reaction between the two native proteins with the ionic strength contribution from sodium phosphate fixed at 0.05 M and the remaining ionic strength provided by KCl; (■) DME-ferrocytochrome b_5 and ferricytochrome c with sodium phosphate as the sole electrolyte. The lines represent nonlinear least-squares fits to the van Leeuwen (1983) relationship. The error in the natural log of the second-order rate constants is less than the size of the symbol.

al. (1984). The diffusion/reaction rate constant is then given by the standard equation:

$$k = 4\pi RDp(b)/\{1 - [1 - p(b)]b/c\} \quad (4)$$

Experimental Results

The absorbance changes monitored for the reduction of ferricytochrome c by ferrocytochrome b_5 at 416 and 428 nm were analyzed as described above to produce second-order rate constants that agreed within 10%. At I = 0.348 M (pH 7.0, 25 °C), the rate of reaction was 1.8 (±0.2) × 10^7 M^{-1} s^{-1} when lumiflavin was used to generate ferrocytochrome b_5. When dithionite was used to produce ferrocytochrome b_5, the rate of reaction was found to be 1.85 (±0.09) × 10^7 M^{-1} s^{-1} under the same conditions. Analysis of the reaction under pseudo-first-order conditions with cytochrome c used in excess produced a second-order rate constant of 2.0 (±0.2) × 10^7 M^{-1} s^{-1}. We conclude from these observations that the use of lumiflavin to reduce cytochrome b_5 for studies employing second-order reaction conditions produces results comparable to those obtained without use of lumiflavin or from pseudo-first-order analysis. Esterification of the cytochrome b_5 heme propionate groups has a minimal effect on the rate of cytochrome c reduction under these same solution conditions, with the second-order rate constant being 1.7 (±0.1) × 10^7 M^{-1} s^{-1}.

The rates of ferricytochrome c reduction by ferrocytochrome b_5 and by DME-ferrocytochrome b_5 demonstrate a marked dependence on ionic strength as illustrated in Figure 2. Interestingly, the native and modified cytochromes b_5 exhibit the same second-order rate constant for reduction of ferricytochrome c at I = 0.4 M (pH 7.0). At lower values of ionic strength, the native protein reacts more rapidly, while at higher ionic strength, the modified derivative is the more efficient reductant. The ionic strength dependence for this reaction is independent of the salt composition used to determine ionic strength. As seen in Figure 2, the ionic strength dependence is the same if sodium phosphate is the sole electrolyte in solution as when the buffer (sodium phosphate) concentration is held constant and the ionic strength is adjusted with KCl.

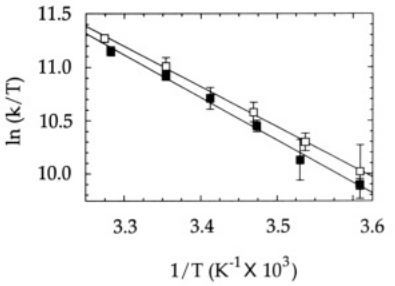

FIGURE 3: Eyring plots of the bimolecular rate constant of ferricytochrome c reduction by native (□) and DME (■)-ferrocytochrome b_5 (I = 0.348 M, pH 7.0). The straight lines represent weighted linear least-squares fit to the data.

The second-order rate constants for ferricytochrome c reduction by either DME- or native ferrocytochrome b_5 were measured at pH 6.0, 6.5, 7.0, 7.5, and 8.0 [I = 0.348 M (sodium phosphate) and 25 °C]. For both forms of cytochrome b_5, the second-order rate constants were independent of pH over this range, with the mean rate constant for reduction of ferricytochrome c by the native protein from pH 6 to 8 being 1.84 (±0.07) × 10^7 M^{-1} s^{-1} and the mean rate constant for reduction by DME-cytochrome b_5 from pH 6 to 8 being 1.55 (±0.07) × 10^7 M^{-1} s^{-1}. The temperature dependence of ferricytochrome c reduction by DME- and native ferrocytochrome b_5 is shown as an Eyring plot in Figure 3 [I = 0.348 M, pH 7.0 (sodium phosphate)]. A weighted linear least-squares analysis of these results yields $\Delta H^{\ddagger}$ = 7.5 (±0.2) kcal/mol and $\Delta S^{\ddagger}$ = −0.3 (±0.6) eu for the reaction between the two native proteins and $\Delta H^{\ddagger}$ = 7.9 (±0.4) kcal/mol and $\Delta S^{\ddagger}$ = 1 (±1) eu for the reduction of ferricytochrome c by DME-ferrocytochrome b_5.

Theoretical Results

Simple Analytical Theories. The simple Smoluchowski (1916) result for two neutral spheres that are completely reactive over their surfaces yields a rate constant k_{Smol} = 7.4 × 10^9 M^{-1} s^{-1}. This rate constant is 1–3 orders of magnitude greater than the experimental values, depending upon the ionic strength. The Smoluchowski result is also independent of ionic strength and pH and makes no prediction of the effect of heme propionate esterification.

The first enhancement of this model is the Smoluchowski–Debye (SD) theory (Debye, 1942), in which the proteins are treated as isotropically reactive spheres with central monopole charges of +7e and −9e, for cytochrome c and cytochrome b_5, respectively. For centrosymmetric forces, the rate constant defined by this model is given by the integral expression:

$$k_{SD} = 4\pi D/\int_R^\infty dr r^{-2} e^{U(r)/k_B T} \quad (5)$$

with $U(r)$ given by eq 2. At pH 7.0 and I = 0.094 M, the rate constant k_{SD} = 1.0 × 10^{10} M^{-1} s^{-1}. This value is even larger than that produced with the assumption of neutral spheres and contains no provision for the stringent steric requirement of the electron-transfer reaction. Furthermore, treatment of the proteins as simple monopoles in this model results in prediction of a relatively weak ionic strength dependence relative to the experimental result, as can be seen in the upper curve in Figure 4.

One might consider improving on the SD theory empirically by multiplying the predicted rate constant by a geometric factor. One means of introducing this parameter is provided by the Schurr and Schmitz (SS) model (Schurr & Schmitz, 1976). The SS model treats the reaction of two neutral

Table IV: Experimental and Brownian Dynamics Simulated Rate Constants ($k \times 10^{-6}$ M^{-1} s^{-1}) as a Function of Ionic Strength for the Exponential and Patch Reaction Criteria Based on both the Computed and Aligned Dipole Models (pH 7.0)[a]

		ionic strength (M)				
	reaction criterion	0.094	0.190	0.286	0.482	0.977
experimental		1250 (100)	80 (7)	30 (2)	11 (4)	4 (1)
computed dipole model	patch (15°, 15°)	310 (80)	100 (30)	85 (20)	50 (20)	40 (6)
	patch (20°, 20°)	710 (120)	260 (30)	190 (40)	110 (10)	100 (10)
	exponential (α = 1.2)	40 (5)	9 (1)	4.9 (0.7)	3.1 (0.6)	2.5 (0.4)
	exponential (α = 1.0)	200 (25)	44 (4)	25 (3)	16 (3)	13.2 (0.2)
	exponential (α = 0.8)	760 (80)	220 (20)	130 (10)	85 (10)	75 (7)
aligned dipole model	patch (5°, 5°)	1250 (100)	350 (50)	170 (20)	60 (10)	17 (10)
	patch (15°, 15°)	1310 (30)	420 (40)	240 (30)	100 (20)	40 (10)
	patch (20°, 20°)	1370 (120)	510 (50)	310 (30)	160 (30)	90 (10)
	exponential (α = 1.2)	660 (90)	90 (10)	31 (4)	9 (3)	4 (10)
	exponential (α = 1.0)	1050 (130)	230 (30)	100 (10)	35 (8)	19 (3)
	exponential (α = 0.8)	1410 (140)	490 (40)	275 (20)	130 (20)	90 (10)

[a] Average deviations are stated in parentheses, α is expressed in units of $Å^{-1}$. Ionic strengths of the KCl buffer set are shown in this table.

particles with axially symmetric reactive patches of small extent to produce an approximate expression for the steric factor f_{ss} defined as follows:

$$k_{ss} = k_{Smol}\theta_1\theta_2(\theta_1 + \theta_2)/8 = k_{Smol}f_{ss} \quad (6)$$

Empirical modification of the SD theory by multiplying by the steric factor f_{ss} simply shifts the theoretical k_{SD} curve down into the range of the experimental rate constants, but it gives the same poor simulation of the observed ionic strength dependence. For example, $f_{ss} = 1.3 \times 10^{-3}$ when $\theta_1 = \theta_2 = 10°$. An improved simulation of the observed ionic strength dependence can only be obtained by complicating the model with a more realistic distribution of protein charges, which we now discuss.

Dipolar Sphere Models. The BD method provides a means of improving the treatment of the electrostatic forces by providing for the steering effect of a more complex charge distribution and by placing a more realistic steric criterion on the reaction. Details of the dipole moment and patch orientations used in the dipolar sphere model are given in Tables I and II. The ionic strength dependence of the rate constants predicted by the patch and exponential reactivity models is shown in Figure 4.

Brownian simulations were performed at pH 7.0 and ionic strengths I = 0.094, 0.190, 0.286, 0.482, and 0.977 M, corresponding to the ionic strengths of the phosphate buffer in which KCl is used to vary I. In the patch model, agreement with experiment at I = 0.094 M and pH 7 is obtained only when the patch sizes are made to be $\theta_{cytc} = \theta_{cytb5} = 20°$ or larger. This assumption is probably not physically realistic, considering that the actual surface area of the proteins in which the heme is exposed gives smaller angles. Furthermore, choosing such large patch angles produces rate constants at I = 0.977 M that are an order of magnitude too large. Conversely, one may choose the high ionic strength regime (I = 0.977 M) to calibrate the patch size parameters of the model, because the effect of Coulombic forces is essentially screened out at this ionic strength. This approach yields a patch size of 10° or less. However, the dipolar steering forces of the model are nonetheless too weak and nonspecific for this model to produce the correct ionic strength dependence, and the BD results fall short of predicting rate constants at the lower ionic strength by an order of magnitude. Nevertheless, the dipole model does predict a greater ionic strength dependence than the simple SD monopole treatment, and in the correct direction, though agreement with experiment remains suboptimal.

The limited enhancement produced by introduction of dipoles into our model suggests several possibilities for improving

Table V: Experimental and Brownian Dynamics Simulated Rate Constants ($k \times 10^{-6}$ M^{-1} s^{-1}) (I = 0.089 M, pH 7.0) Showing the Effects of Cytochrome b_5 Heme Propionate Esterification[a]

	native	DME	k_{DME}/k_{native}
experimental	540 (90)	160 (30)	0.30
patch, computed dipole (20°, 20°)	750 (50)	310 (40)	0.41
patch, aligned dipole (5°, 5°)	1350 (75)	460 (50)	0.34
exponential, computed dipole (α = 1.2)	49 (4)	8.4 (0.9)	0.17
exponential, aligned dipole (α = 1.2)	760 (60)	140 (20)	0.18

[a] Average deviations are stated in parentheses, α is expressed in units of $Å^{-1}$. The results obtained with the lowest ionic strength of the all-phosphate buffer set are shown.

the model that are discussed below. The first possibility is that the computed dipole vectors do not coincide with the true dipole moment of the proteins because of the various approximations made in assigning charges. We have seen by experience that the dipole direction and magnitude are quite sensitive to small changes in the charge locations and magnitudes (Northrup et al., 1986b). The true dipole may, in fact, be more closely correlated with the electron-transfer region than the ~30–40° displacement angle that we have seen in these computations. The second possibility is that the dipole model may be adequate to emulate the electrostatic properties of these proteins at large distances but inadequate to capture the realism of the local charge distribution near the reactive surfaces. As seen in studies of the cytochrome *c*–cytochrome *c* peroxidase reaction, the diffusional association rates seem to correlate more closely with local charge effects than with global electrostatic properties such as net monopole and dipole (Northrup et al., 1987a,b). The third possibility is that the extended Debye–Hückel theory, empirically modified here to include noncentrally imbedded charges, may not adequately describe the electrostatics at these high values of ionic strength. While this is perhaps true, it probably would not explain the order of magnitude discrepancy observed between theory and experiment at I = 0.094 M when the patch model is calibrated to fit the results obtained at I = 0.977 M. Past studies (Northrup et al., 1987a,b) have shown that the effects of various electrostatic treatments on the rate constants are much smaller than this.

To test the more likely first and second hypotheses, we examined a dipolar model in which (1) the dipole vector is perfectly aligned with the electron-transfer region and (2) smaller, more realistic patch sizes are employed that give closer correspondence at high ionic strength. While this *aligned dipole* model departs from the compound electrostatic dipolar properties of the proteins, it captures the realism of having

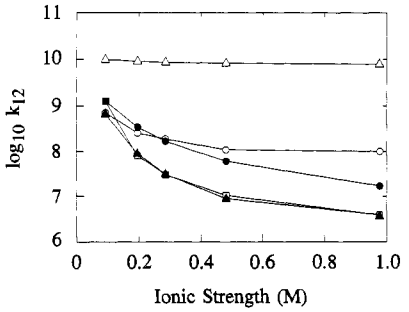

FIGURE 4: Log of the electron-transfer rate constant for reaction between cytochrome c and cytochrome b_5 at pH 7 versus I showing results for the experimental values (□), the simple Smoluchowski–Debye theory (△), and the BD-simulated results for the reactive patch model with patch sizes (20°, 20°) in the computed dipole case (○), reactive patch angle choice (5°, 5°) in the aligned dipole case (●), and the exponential reactivity model with aligned dipoles at α = 1.2 Å^{-1} (▲).

a local concentration of charges around the electron-transfer surfaces that greatly favor the reaction and provide more direct steering and locking than the computed dipoles. Results of calculations based on this model are given in Table V. In Figure 4, we see that concentrating the dipolar charges on the reaction site does, in fact, produce a somewhat more reasonable ionic strength dependence throughout the experimental regime and produces fair correlation with experiment at I = 0.1 M when $\theta_{cytc} = \theta_{cytb5} = 5°$ or less. We have not made an extended attempt to find combinations of parameters that produce an exact fit to the experimental results with the patch model but were primarily interested in exploring the properties of simple idealized models that resemble the system of interest. Our study does show, however, that the simple dipole model using the computed dipoles at tens of degrees from the reaction center produces an ionic strength dependence that is too weak. The aligned dipole model predicts better ionic strength dependence either because the true dipoles are more closely aligned with the reaction site than we predict or because this dipole model more accurately emulates the steering effects of the local charge distribution.

The results generated by the exponential distance-dependent reactivity model produce substantially better agreement with experiment than results produced by the reactive patch model just described. In the exponential model, the electron-transfer distance parameter α takes the place of the patch angle θ as a measure of the extent of the reactive region. The larger the α value, the smaller the extent of distance-dependent reactivity. McLendon (1988) and co-workers and Northrup and Herbert (1989) have both estimated values of α = 1.2 Å^{-1} for these types of systems, the latter study involving BD simulations of electron self-exchange in *Pseudomonas aeruginosa* cytochrome c_{551}. Results for the exponential model are given in Figure 4 and Table IV. The exponential model predicts an ionic strength dependence for the reduction of ferricytochrome c by ferrocytochrome b_5 that is virtually identical with that observed experimentally when the aligned dipole model is employed. Furthermore, a realistic value of α = 1.2 Å^{-1} again produces the fit to experiment, just as found in previous studies.

Effects of Ferricytochrome b_5 Heme Propionate Esterification. We employed the dipolar sphere model with both computed and aligned dipoles, and with patch and exponential reactivity models to predict the electrostatic effect of removal of the negatively charged heme propionate groups of cytochrome b_5 on the reaction rate of this modified protein with ferricytochrome c. BD simulations of derivatives were performed at pH 7 and I = 0.089 M, corresponding to the lowest ionic strength studied using the all-phosphate buffer. This derivative (DME-cytochrome b_5) was emulated by recomputing the net monopole and dipole with the heme propionate charges set to zero. The negative end of the dipole moment of cytochrome b_5 became further misaligned from the electron-transfer region (Fe vector) upon esterification, changing from 38° to 50° on esterification, and the dipole magnitude decreased from 638 to 517 D. Thus, the rate of DME-ferrocytochrome b_5 reaction with ferricytochrome c is expected to decrease from that observed with native ferrocytochrome b_5 through two effects: a diminished monopole attraction, and a diminished dipole alignment and strength. The predicted effect of heme propionate esterification on reaction rate (Table V) can be expressed by the ratio $x = k_{dme}/k_{native}$. For the original computed dipole model with patch sizes of 20°, the rate constant decreased from 7.50 × 10^8 to 3.10 × 10^8 M^{-1} s^{-1} (x = 0.41), compared to a more substantial experimental drop from 5.40 × 10^8 to 1.60 × 10^8 M^{-1} s^{-1} (x = 0.30). Comparable results were obtained by using the exponential reaction model with α = 1.2 Å^{-1}. The derivatization effect was included in the case of the aligned dipole model by moving the dipole from perfect alignment with the electron-transfer region to 12° from perfect alignment, as computed. Overall, the theoretical results indicate that the effect of esterification on the rates can at least be rationalized on the basis of the perturbation in the electrostatic properties of cytochrome b_5.

Modeling the pH Dependence. To simulate the effect of pH on the reaction between the two native cytochromes, the first step was to perform Tanford–Kirkwood calculations at each value of pH studied to calculate the protonation state changes of titratable amino acid residues in the two cytochromes and then to calculate the changes in net monopole and dipole of the two proteins as a function of pH. These monopole and dipole values were then used in BD simulations to compute the expected rate constants at each pH. Table II shows how the computed net monopole and dipole changes with pH at the ionic strength I = 0.482 M at which the experimental study was performed. As pH changes from 6.0 to 8.0, the net charge of cytochrome c decreases from +8.4e to +6.5e, and the net charge of cytochrome b_5 decreases from −7.3e to −10.5e. These changes in protein charge are largely attributable to changes in the protonation status of the α-amino group and histidyl residues. DME-cytochrome b_5 behaves similarly to the native protein but at roughly +2e charge units greater than the native protein. The monopole–monopole potential energy term at contact separation between proteins becomes slightly more attractive at I = 0.482 M as the pH varies from 6.0 (−1.9 kcal/mol) to 8.0 (−2.1 kcal/mol), indicating a small effect of pH on the association rate constant. We also computed a modest variation in the magnitude and direction of the dipole moments of these proteins between pH 6.0 and 8.0 as shown in Table II. The dipole moments of cytochrome c, cytochrome b_5, and DME-cytochrome b_5 changed roughly 10% in magnitude and changed by several degrees in angle in response to variation in pH. The magnitude of the cytochrome c dipole increased, while those of DME- and native cytochrome b_5 decreased. The dipoles of all three proteins became less aligned with the electron-transfer region as pH increased. All changes in the electrostatic properties were sufficiently modest that little pH dependence of the rate constant is expected based purely on these considerations. This is, in fact, what is observed both in experiment and in the BD simulations as illustrated in Table VI. A very slight increase in k is observed in experiment, while the simulated rate constant does not vary outside of the range of its own statistical uncertainty.

Table VI: Brownian Dynamics Simulated Rate Constants ($k \times 10^{-6}$ M^{-1} s^{-1}) as a Function of pH (I = 0.486 M)[a]

reaction	case	pH 6.0	pH 6.5	pH 7.0	pH 7.5	pH 8.0
cytochrome c–cytochrome b_5	exponential model (α = 1.2)	3.7 (0.6)	3.6 (0.7)	3.1 (0.6)	3.3 (0.4)	3.0 (0.3)
	exponential model (α = 1.0)	18 (2)	18 (3)	16 (3)	17 (2)	15 (2)
	patch (computed dipole) (20°, 20°)	150 (30)	130 (20)	110 (10)	130 (20)	130 (30)
	patch (aligned dipole) (5°, 5°)	55 (20)	70 (20)	60 (10)	50 (20)	40 (10)
cytochrome c–DME-cytochrome b_5	exponential model (α = 1.2)	2.6 (0.3)	2.5 (0.4)	2.7 (0.3)	2.8 (0.5)	2.7 (0.3)
	exponential model (α = 1.0)	13 (2)	13 (2)	14 (1)	14 (2)	14 (1)
	patch (computed dipole) (20°, 20°)	130 (20)	110 (15)	110 (20)	120 (20)	110 (20)
	patch (aligned dipole) (5°, 5°)	10 (10)	16 (7)	10 (10)	14 (7)	12 (5)

[a] Average deviations are stated in parentheses, α is expressed in units of $Å^{-1}$.

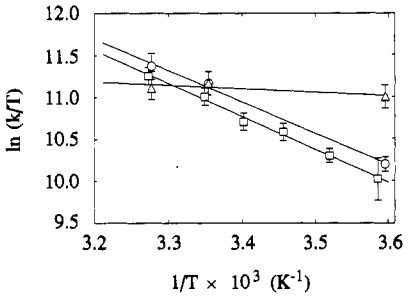

FIGURE 5: Arrhenius plot of the temperature dependence of the bimolecular reaction rate constant for reduction of ferricytochrome c by ferrocytochrome b_5 [pH 7, I = 0.348 M (phosphate)]. (□) Experimental rate constants; (○) rate constants predicted by the exponential model with the aligned dipole assumption, α = 1.2 $Å^{-1}$, and the temperature-dependent intrinsic k_{et} given by eq 7 with $\Delta H_{et}^{\ddagger}$ = 6.55 kcal/mol; (△) rate constants predicted by the same exponential model, but with a temperature-independent k_{et}.

Modeling the Temperature Dependence. As the best theoretical simulation of the experimental ionic strength dependence was obtained by incorporating the exponential model (including the intrinsic electron-transfer rate constant having exponential distance behavior) and aligning the dipoles with the region of electron transfer, we focused on this model to study the temperature dependence as well. First, we assumed the intrinsic k_{et} constant to be completely temperature independent to see if the temperature dependence was manifested in the diffusional stage of the reaction alone. In this case, the most significant parameter affecting the bimolecular rate constant is the change in diffusion coefficients, which vary as $D \sim T/\eta$. Only minor temperature dependences are manifested in the dielectric constant of the medium, the reciprocal Debye screening length κ, and the protonation status of titratable groups on the protein. Simulations were performed at 278.15, 298.15, and 305.15 K, and the results are plotted as ln (k/T) versus $1/T$ in Figure 5 along with the experimental rate constants. The slopes of these linear least-squares fits reflect the activation enthalpy of the reaction, $\Delta H^{\ddagger}$, which has an experimental value of 7.5 kcal/mol and a value predicted by this model of only 0.78 kcal/mol. Obviously, the temperature dependence is not well represented by the exponential model in which the intrinsic electron-transfer rate constant is independent of temperature. This finding signifies that the bulk of the temperature dependence lies in the electron-transfer rate constant.

It is interesting to note that even in a purely diffusion-controlled reaction between two neutral or oppositely charged spheres that react instantaneously upon contact, the temperature dependence in the diffusion coefficients alone gives rise to an effective $\Delta H^{\ddagger} \sim 4$ kcal/mol. It is, therefore, reasonable to question why this activation enthalpy is not predicted by the exponential model of these proteins. This result is not obtained because for the exponential model, the rate of reaction depends not only on how fast the proteins diffuse to the reaction site but also on the length of time that the reactants remain in this position for reaction to occur according to k_{et}. Although lowering the temperature retards the rate of diffusion to the reactive region, which lowers the reaction rate, the lifetime of the reactants in this region is enhanced by the concomitant decrease in rate of dissociation of the protein–protein complex. It is for this reason that the effective $\Delta H^{\ddagger}$ using the exponential model is much less than 4 kcal/mol and, in fact, virtually zero.

Therefore, it is appropriate to study a second model in which the preexponential factor of the k_{et} rate constant given by eq 3 is considered to be dependent on temperature according to an Arrhenius model:

$$k_{et}(r_0, T) = cTe^{-\Delta H_{et}^{\ddagger}/RT} \quad (7)$$

Here, the activation entropy and other microscopic parameters are contained in the c term, with the temperature dependence displayed through the T prefactor and exponential term. The constant c is chosen such that $k_{et}(r_0, 298.15) = 1.0 \times 10^{11}$ s^{-1} ($c = 2.1 \times 10^{13}$ s^{-1} K^{-1}) consistent with the other BD simulations of the exponential model at T = 298.15 K. Employing an activation enthalpy for the intrinsic ET step of $\Delta H_{et}^{\ddagger}$ = −6.55 kcal/mol, we achieve an excellent fit to the experimental temperature dependence as shown in Figure 5 and obtain an overall activation enthalpy of reaction of 7.5 kcal/mol. Thus, our BD model is able in principle to resolve the activation enthalpy of the overall reaction into diffusional and chemical contributions.

Discussion

The reduction of ferricytochrome c by ferrocytochrome b_5 occurs with a second-order rate constant that is large in comparison with rate constants reported for reactions between other small electron-transfer proteins. Many electron-transfer protein reactions exhibit bimolecular kinetics at physiologically relevant ionic strengths and higher. Bimolecular rates manifest not only the intrinsic redox capabilities of these metalloproteins, as ordinarily studied in complexed states at low ionic strength or in covalently cross-linked complexes, but also can often manifest the important coupling to diffusion effects. In the diffusional association stage of reaction, the translating and rotating proteins are sensitive to electrostatic steering effects that act over long ranges. More importantly, the proteins are thought to explore a wide variety of mutual orientations in a single encounter by somewhat nonspecific hydrophobic and ionic interactions, and a large number of casual precursor complexes are sampled before an intimate complex capable of electron transfer is obtained (Northrup et al., 1988). The dynamics of this type of interaction scenario will play a major role in determining the overall electron-transfer kinetics, especially when electron-transfer proteins react with second order at very large rates, as in the present example under study. The present analysis considers several mechanistic features of the

Table VII: Thermodynamic Parameters for Several Bimolecular Protein–Protein Electron-Transfer Reactions

reactants[k]	$\Delta H^{\ddagger}$ (kcal/mol)	$\Delta S^{\ddagger}$ (eu)	reference
ferrocytochrome f + cupriplastocyanin[d,f]	10.5	11.0	Wood (1974)
ferrocytochrome f + cupriplastocyanin[b,g]	8.4	4.9	Niwa et al. (1980)
ferricytochrome f + cuproplastocyanin[b,g]	8.6	3.9	Niwa et al. (1980)
ferrocytochrome f + cupriplastocyanin[h]	13.4	21.5	Tanaka et al. (1981)
ferrocytochrome c + cupriplastocyanin[a]	7.6	−2.4	King et al. (1985)
ferrocytochrome c_{551} + cupriazurin[c,i]	7.8	−1.1	Rosen & Pecht (1976)
ferricytochrome c_{551} + cuproazurin[c,i]	13.7	18.8	Rosen & Pecht (1976)
ferrocytochrome c_{551} + cupriazurin[d,j]	18.1	31.0	Rosen et al. (1981)
ferricytochrome c_{551} + cuproazurin[d,j]	15.2	22.5	Rosen et al. (1981)
ferrocytochrome c + ferricytochrome c	8.4	−11	Barbush & Dixon (unpublished results)
ferrocytochrome b_5 + ferricytochrome b_5[d]	5.5	−23	Dixon et al. (1990)
ferrocytochrome b_5 + ferricytochrome c[e]	7.5	−0.3	this work
DME-ferrocytochrome b_5 + ferricytochrome c[e]	7.9	1.0	this work

[a] I = 0.1 M, pH 7.5. [b] I = 0.2 M, pH 7.0. [c] I not stated, pH 7.0. [d] I = 0.1 M, pH 7.0. [e] I = 0.5 M, pH 7.0. [f] *Petroselinum sativum.* [g] *Brassica komatsuno.* [h] *Raphanous sativus.* [i] *Pseudomonas aeruginosa.* [j] *Alcaligenes faecalis.* [k] In those instances where the errors in the thermodynamic activation parameters are reported, they are not greater than 1 unit. Footnotes *a–e* refer to solution conditions while footnotes *f–j* refer to the source of protein isolated from nonmammalian tissues.

reaction between these two proteins that contribute to this rate and to its variation with solution conditions.

The unimolecular rate constant of electron transfer from cytochrome b_5 to cytochrome c has been determined by pulse radiolysis to be 1600 (±700) s^{-1} (1 mM phosphate, pH 7) (McLendon & Miller, 1985). If electron transfer between the heme groups within the cytochrome b_5–cytochrome c complex is comparable at 1 mM phosphate and I = 0.348 M, and if ferrocytochrome b_5 reduction of cytochrome c involves a protein–protein binding step prior to electron transfer, then at I = 0.348 M, pH 7, the association constant of ferrocytochrome b_5 and ferricytochrome c is $\sim 10^4$ M^{-1}. This value is larger than experimentally determined values (e.g., 10^3 M^{-1} measured at I = 0.04 M) (Eley & Moore, 1983), suggesting that the rate of electron transfer within the protein–protein complex is ionic strength dependent. Hazzard et al. (1988) have previously observed that the rate of electron transfer within the cytochrome c–cytochrome c peroxidase complex does exhibit a dependence on ionic strength.

As expected for a reaction between oppositely charged reactants, the rate of reaction varies inversely with ionic strength. The lines in Figure 2 represent unweighted fits of the experimental data to the van Leeuwen (1983) equation using radii and dipole moments for each protein given in Tables I and III. The second-order rate constants for the reduction of ferricytochrome c by ferrocytochrome b_5 at infinite ionic strength predicted by these analyses are 5 (±5) × 10^5 and 4 (±1) × 10^6 M^{-1} s^{-1}, respectively. The product of the net monopole charges on the proteins required to fit the data is −210 and −170, respectively. The poor agreement between these results and the charge product expected from analysis of the structures of the two proteins probably relates to the inappropriate application of the van Leeuwen relationship to analysis of rate studies conducted at high ionic strength and indicates that an alternative model such as our BD model is required to represent the ionic strength dependence of these reactions. We note, nonetheless, that Dixon and colleagues have obtained acceptable results in the analysis of the ionic strength dependence of cytochrome electron-transfer self-exchange rate constants with the van Leeuwen relationship (Dixon et al., 1989, 1990; Dixon & Hong, 1990).

The activation parameters for ferricytochrome c reduction by native and DME-ferrocytochrome b_5 are very similar (I = 0.348 M, pH 7.0). With the notable exception of self-exchange reactions, the activation enthalpy and entropy of ferrocytochrome b_5 reduction of ferricytochrome c fall within the values measured for other bimolecular protein–protein electron-transfer reactions (cf. Table VII). While the activation enthalpy of ferrocytochrome b_5 reduction of ferricytochrome c is comparable to that of the bimolecular oxidation or reduction of either cytochromes b_5 (Reid & Mauk, 1982; Reid et al., 1984) or c (Hodges et al., 1974; Cummins & Gray, 1977; Mauk et al., 1979) with a variety of small electron-transfer reagents, the activation entropy of the protein–protein reaction is considerably larger than those of the protein–reagent reactions. This result suggests that the principal reason that the rate of electron transfer between cytochromes b_5 and c exceeds the rate of electron transfer between each of these proteins and small reagents is that the activation entropy of the protein–protein electron-transfer reaction is much greater. The large, negative activation entropies of electron transfer between small reagents and proteins have been partly explained in terms of the loss of translational and rotational degrees of freedom accompanying formation of the collisional complex of the reactants (Bennett, 1973) and have been estimated to be about 13 eu. It is possible that in the case of ferrocytochrome b_5 reduction of ferricytochrome c, these entropic losses could be compensated by the release of solvent molecules at the protein–protein interface in complex formation (Chothia & Janin, 1975; Mauk et al., 1982).

The rate of ferrocytochrome b_5 reduction of (trifluoromethyl)phenylcarbamyl-Lys-13 cytochrome c has been measured to be ~37% that of native ferricytochrome c at 0.1 M ionic strength (Ng et al., 1977), but at I = 1.5 M, the two forms of cytochrome c are reduced at the same rate by ferrocytochrome b_5 (Stonehuerner et al., 1979). Although the rate constant that these workers report is estimated from steady-state kinetics and was not measured directly, the ionic strength dependence that they report is similar to that observed in the present study. It is also intriguing that cytochrome c lysine modifications that decreased this rate the most at I = 0.1 M (Lys-13, Lys-72) exhibited rate constants that where 35–40% that of native cytochrome c (Stonehuerner et al., 1979). In the present study, ferricytochrome c reduction by DME-ferrocytochrome b_5 (I = 0.089) yielded a rate constant that is 70% smaller than that of ferricytochrome c reduction by native ferrocytochrome b_5. While DME-cytochrome b_5 is modified at two positions, these results are consistent with the involvement of cytochrome b_5 heme propionate-6 in stabilizing the cytochrome b_5–cytochrome c complex to the same extent as cytochrome c lysines-13 and -72. This result is compatible with the model of the cytochrome b_5–cytochrome c complex proposed by Salemme (1986).

A combination of electrostatic analysis and BD simulation has been used to predict the ionic strength, temperature, and pH dependence of the rate of bimolecular electron transfer

from ferrocytochrome b_5 to ferricytochrome c, taking into account the coupling of electrostatics and diffusional effects. Both proteins are highly charged species and of opposite sign (ca. +7e and −9e for ferricytochrome c and ferrocytochrome b_5, respectively). The net monopole–monopole attraction is supplemented by an important dipolar attraction in which the positive end of the dipole of cytochrome c passing near the exposed heme edge is attracted to the monopole of cytochrome b_5 as well as the negative end of the cytochrome b_5 dipole, which is near the exposed heme region of cytochrome b_5. In the center of mass reference frame, the dipole vector of cytochrome c makes only a 30.5° angle with respect to the position vector of the Fe atom and has a magnitude of 284 D at pH 7 and I = 0.094 M. In cytochrome b_5, the negative end of the dipole vector also makes a 37.8° angle with respect to the position vector of the Fe atom and has a magnitude of 638 D under the same conditions.

Ionic strength dependence studies provide a meaningful probe of the electrostatic influences of reactions. In the BD simulations, we have confirmed that the large Coulombic attractive forces between these species are necessary to provide for the large association rate constant observed in experiment, as well as the observed negative ionic strength dependence of the bimolecular rate. However, BD simulation results have shown that the net charges alone do not enhance the association rate sufficiently to provide for the steep negative ionic strength dependence or to offset the retarding effect of the orientational constraints for electron transfer. Additional significant electrostatic enhancement in this reaction results from, at least in part, the large dipole moments on both proteins. The BD method has provided a means of improving on simple analytical theories by providing for a more complex charge distribution and enforcing a stringent steric criterion on the reaction. In this work, we have used a simple spherical dipole model of the proteins. Though we have performed more robust BD simulations in other systems (Northrup et al., 1986b, 1987a,b, 1988), the computational efficacy of the simple model has enabled us to explore a wide variety of solution conditions. Although the BD spherical dipole model does give a stronger ionic strength dependence than the simple monopole terms alone, and in the correct direction, the added dipolar steering forces of the model are still too weak and nonspecific to produce the correct ionic strength dependence. The implications of this result are 2-fold: either (i) the computed dipole vectors do not coincide with the true dipole moment of the proteins because of the various approximations in assigning charges or (ii) a model consisting of monopoles and dipoles only is inadequate to capture the realism of the local charge distribution near the reactive surfaces. The latter possibility has been borne out in BD studies of the reaction between ferrocytochrome c and cytochrome c peroxidase (Northrup et al., 1986b, 1987a,b, 1988) that showed that the diffusional association rates more closely correlate with local charge effects than with global electrostatic properties such as net monopole and dipole. To test this hypothesis again in the context of this reaction, we constructed an alternative aligned dipole model in which the dipole vectors are perfectly aligned with the electron-transfer region. This model, while it departs from the computed electrostatic dipolar properties, captures the realism of having a local concentration of charges around the electron-transfer surfaces which highly favor the reaction and provide more direct steering and docking than the computed dipoles. Concentrating the dipolar charges on the reaction site does in fact give the correct ionic strength dependence throughout the experimental regime and gives excellent correlation with experiment with more realistic steric criteria, especially with the exponential distance dependent model of ET.

Site-specific mutation and chemical derivatization of charged groups provide yet another probe of the mechanism responsible for the large bimolecular rates observed in this reaction. We have employed the dipolar sphere model with both computed and aligned dipoles to predict the effect of esterification of the two charged heme propionates on the ferrocytochrome b_5. By electrostatic analysis, we expected the reaction rate of the derivative to decrease from the native species by two effects: a diminished monopole attraction and a diminished dipole alignment and strength. For the original computed dipole model with patch sizes of 20° at I = 0.089 M and pH 7.0, the theoretical rate constant decreased from 7.50×10^8 to 3.10×10^8 M^{-1} s^{-1} compared to an experimental drop from 5.40×10^8 to 1.57×10^8 M^{-1} s^{-1}. Although the dipolar sphere simulation predicts the correct direction of the effect, the quantitative effect of derivatization cannot be predicted simply by the change in global electrostatic properties of the protein. The proteins most likely take advantage of more specific sorts of charge complementarity than can be reproduced by a monopole/dipole representation, or there are additional steric effects on the reactivity, or additional changes in the redox properties of this pair of proteins are involved.

The pH dependence of the bimolecular rate has been studied theoretically by performing repeated Tanford–Kirkwood calculations at different values of pH using the computed changes in charge status to modify the net monopoles and dipoles of the proteins. As Table II indicates, the monopole–monopole charge product changes only slightly from pH 6.0 to 8.0, and the magnitude and direction of the dipole moments of these proteins vary only modestly. All changes in the electrostatic properties were sufficiently modest that little pH dependence of the BD-simulated rate constant was obtained, as borne out by experiment.

In all previous BD simulation studies, the chemical reaction event has been treated as a "black box" and taken to occur instantaneously upon collision of certain geometric surfaces. In essence, the diffusion away from a collision event is assumed to be slow on the time scale of the reactive event. This assumption is implicit in the patch model employed here. Thus, the conventional BD result is only a theoretical upper bound estimate to the true bimolecular rate because it does not take into account additional retardation of the rate attributable to a chemical activation step. Consequently, important factors in electron transfer such as the electromotive driving force, reorganization energy, etc. have not been accounted for in any explicit fashion. To remedy this situation, we have taken a beginning step in this study by explicitly incorporating the rate constant for the intrinsic electron-transfer step into the BD simulation method through the exponential distance-dependent model. This provides at least an initial framework for the dynamic coupling between the diffusional association event and a noninstantaneous electron-transfer event. The rate constant for electron transfer has taken the form $A \exp(-\alpha r)$, with the spatial dependence in the exponential term and all other microscopic factors entering through the amplitude A. In principle, it should be possible in future studies to vary A between various species and mutants to account for changes in driving force and other features. Such was not done here.

In the exponential model, the electron-transfer distance parameter α essentially takes the place of the patch angle θ as a measure of reactive region extent. Previous studies (Marcus & Sutin, 1985; Mayo et al., 1986; McLendon, 1988;

Northrup & Herbert, 1989) have estimated values of $\alpha = 1.2$ Å^{-1} for these types of systems, the latter study being in the context of BD simulations of electron self-exchange in *Pseudomonas aeruginosa* cytochrome c_{551}. Unlike the patch model, the exponential model gives an ionic strength dependence that correlates well with experiment. Values of $\alpha = 1.2$ Å^{-1} and the employment of aligned dipoles gave excellent agreement with experiment throughout the ionic strength range. It is significant that our exponential electron-transfer rate constant did in fact give us the necessary retardation of the rate at high ionic strengths to provide a closer fit to the experiment than was possible with the patch model. This is because, in the exponential model, the overall reaction rate no longer depends only on how fast and with what probability the particles diffuse to the correct reaction geometry but also on *how long they persist in the region.* Such dynamic information does not enter into an "all-or-nothing" geometric model of reactivity. At high ionic strengths, the lifetime of the properly oriented pairs is diminished. This reaction thus appears not to be purely at the diffusion-controlled limit but is partially diffusion-controlled, and the chemical activation control portion of the rate is embodied in the electron-transfer rate constant k_{et}.

Our theoretical analysis indicates that the temperature dependence is not manifested in the diffusion step but in the intrinsic electron-transfer rate constant. Simulations are currently underway to compute the bimolecular rate constants and docking orientation profiles of this reaction pair using lengthy BD calculations with atomic-scale resolution and Poisson–Boltzmann-generated potentials. These calculations should be able to predict the effects of propionate esterification and site-directed mutations more quantitatively and to provide better correspondence with experiment without the extensive parameterization of the simple dipolar sphere model.

ACKNOWLEDGMENTS

We thank Professor Gary Brayer for providing the atomic coordinates for horse heart cytochrome c prior to publication. S.H.N. thanks Christine Northrup for secretarial assistance, Dr. James Matthew for providing computer programs to implement the Tanford–Kirkwood formalism, and Professors Stuart Allison, Dabney Dixon, and Andrew McCammon for helpful discussions.

Registry No. Cytochrome c, 9007-43-6; cytochrome b_5, 9035-39-6.

REFERENCES

Allison, S. A., Northrup, S. H., & McCammon, J. A. (1985) *J. Phys. Chem. 83*, 2894.
Argos, P., & Mathews, F. S. (1975) *J. Biol. Chem. 250*, 747.
Bennett, L. E. (1973) *Prog. Inorg. Chem. 18*, 1.
Berman, M. C., Adnams, C. M., Ivanetich, K. M., & Kench, J. E. (1976) *Biochem. J. 157*, 237.
Bernstein, F. C., Koetzle, T. F., Williams, G. J. B., Meyer, E. F., Jr., Brice, M. D., Rodgers, J. R., Kennard, O., Shimanouchi, T., & Tasumi, M. (1977) *J. Mol. Biol. 112*, 535.
Brautigan, D. L., Ferguson-Miller, S., & Margoliash, E. (1978) *Methods Enzymol. 53*, 128.
Bushnell, G., Louie, G. V., & Brayer, G. D. (1990) *J. Mol. Biol. 214*, 585.
Chapman, S. K., Davies, D. M., Vuik, C. P. J., & Sykes, A. G. (1984) *J. Am. Chem. Soc. 106*, 2692.
Chothia, C., & Janin, J. (1975) *Nature 256*, 705.
Cummins, D., & Gray, H. B. (1977) *J. Am. Chem. Soc. 99*, 5158.
Debye, P. (1942) *Trans. Electrochem. Soc. 82*, 265.
Dickinson, E. (1985) *Chem. Soc. Rev. 14*, 421.
Dixon, D. W., & Hong, X. (1990) *Adv. Chem. Ser. 226*, 162.
Dixon, D. W., Hong, X., & Woehler, S. E. (1989) *Biophys. J. 56*, 339.
Dixon, D. W., Hong, X., Woehler, S. E., Mauk, A. G., & Sishta, B. P. (1990) *J. Am. Chem. Soc. 112*, 1082.
Eley, G. C. S., & Moore, G. R. (1983) *Biochem. J. 215*, 11.
Eltis, L. D. (1989) Ph.D. Dissertation, University of British Columbia.
Ermak, D. L., & McCammon, J. A. (1978) *J. Chem. Phys. 69*, 1352.
Funk, W. D., Lo, T. P., Mauk, M. R., Brayer, G. D., MacGillivray, R. T. A. M., & Mauk, A. G. (1990) *Biochemistry 29*, 5500.
Gray, H. B. (1986) *Chem. Soc. Rev. 15*, 17.
Guarr, T., McGuire, M., Strauch, S., & McLendon, G. L. (1983) *J. Am. Chem. Soc. 105*, 616.
Hartshorn, R. T., Mauk, A. G., Mauk, M. R., & Moore, G. R. (1987) *FEBS Lett. 213*, 321.
Harvey, S. C. (1989) *Proteins: Struct., Funct., Genet. 5*, 78.
Hazzard, J. T., Poulos, T. L., & Tollin, G. (1987) *Biochemistry 26*, 2836.
Hazzard, J. T., McLendon, G., Cusanovich, M. A., & Tollin, G. (1988) *Biochem. Biophys. Res. Commun. 151*, 429.
Hodges, H. L., Holwerda, R. A., & Gray, H. B. (1974) *J. Am. Chem. Soc. 96*, 3132.
Hoffman, B. M., & Ratner, M. A. (1987) *J. Am. Chem. Soc. 109*, 604.
King, G. C., Binstead, R. A., & Wright, P. E. (1985) *Biochim. Biophys. Acta 806*, 262.
Koppenol, W. H., & Margoliash, E. (1982) *J. Biol. Chem. 257*, 4426.
Lamm, G., & Schulten, K. (1983) *J. Chem. Phys. 78*, 2713.
Leung, P.-S. K., Betterton, E. A., & Hoffman, M. R. (1989) *J. Phys. Chem. 93*, 430.
Marcus, R. A., & Sutin, N. (1985) *Biochim. Biophys. Acta 811*, 265.
Margoliash, E., & Frohwirt, N. (1959) *Biochem. J. 71*, 570.
Matthew, J. B. (1985) *Annu. Rev. Biophys. Biophys. Chem. 14*, 387.
Mauk, A. G., Coyle, C. L., Bordignon, E., & Gray, H. B. (1979) *J. Am. Chem. Soc. 101*, 5054.
Mauk, M. R., Reid, L. S., & Mauk, A. G. (1982) *Biochemistry 21*, 1843.
Mauk, M. R., Mauk, A. G., Weber, P. C., & Matthew, J. B. (1986) *Biochemistry 25*, 7085.
Mayo, S. L., Ellis, W. R., Crutchley, R. J., Jr., & Gray, H. B. (1986) *Science 233*, 948.
McLendon, G. L. (1988) *Acc. Chem. Res. 21*, 160.
McLendon, G. L., & Miller, J. R. (1985) *J. Am. Chem. Soc. 107*, 7811.
McLendon, G. L., Winkler, J. R., Nocera, D. G., Mauk, M. R., Mauk, A. G., & Gray, H. B. (1985) *J. Am. Chem. Soc. 107*, 739.
Moore, G. R., Eley, G. C. S., & Williams, G. (1984) *Adv. Inorg. Bioinorg. Mech. 3*, 1.
Ng, S., Smith, M. B., Smith, H. T., & Millett, F. (1977) *Biochemistry 16*, 4975.
Niwa, S., Ishikawa, H., Nikai, S., & Takabe, T. (1980) *J. Biochem. 88*, 1177.
Northrup, S. H., & Herbert, R. G. (1989) *J. Mol. Liq. 41*, 207.
Northrup, S. H., Pear, M. R., Morgan, J. D., McCammon, J. A., & Karplus, M. (1981) *J. Mol. Biol. 153*, 1087.
Northrup, S. H., Allison, S. A., & McCammon, J. A. (1984) *J. Chem. Phys. 80*, 1517.

Northrup, S. H., Curvin, M., Allison, S. A., & McCammon, J. A. (1986a) *J. Chem. Phys. 84*, 2196.
Northrup, S. H., Reynolds, J. C. L., Miller, C. M., Forrest, K. J., & Boles, J. O. (1986b) *J. Am. Chem. Soc. 108*, 8162.
Northrup, S. H., Boles, J. O., & Reynolds, J. C. L. (1987a) *J. Phys. Chem. 91*, 5991.
Northrup, S. H., Luton, J. A., Boles, J. O., & Reynolds, J. C. L. (1987b) *J. Comput.-Aided Mol. Des. 1*, 291.
Northrup, S. H., Boles, J. O., & Reynolds, J. C. L. (1988) *Science 241*, 67.
Ozols, J., & Strittmatter, P. (1964) *J. Biol. Chem. 239*, 1018.
Pielak, G. J., Mauk, A. G., & Smith, M. (1985) *Nature 313*, 152.
Reid, L. S., & Mauk, A. G. (1982) *J. Am. Chem. Soc. 104*, 841.
Reid, L. S., Mauk, M. R., & Mauk, A. G. (1984) *J. Am. Chem. Soc. 106*, 2182.
Reynolds, J. C. L., Cooke, K. F., & Northrup, S. H. (1990) *J. Phys. Chem. 94*, 985.
Rosen, P., & Pecht, I. (1976) *Biochemistry 15*, 775.
Rosen, P., Segal, M., & Pecht, I. (1981) *Eur. J. Biochem. 120*, 339.
Salemme, F. R. (1976) *J. Mol. Biol. 102*, 563.
Schurr, J. M., & Schmitz, K. S. (1976) *J. Phys. Chem. 80*, 1934.
Scott, R. A. (1979) Ph.D. Dissertation, California Institute of Technology.
Sharp, K., Fine, R., & Honig, B. (1987a) *Science 236*, 1460.
Sharp, K., Fine, R., & Schulten, K. (1987b) *J. Phys. Chem. 91*, 3624.
Shire, S. J., Hanania, G. I. H., & Gurd, F. R. N. (1974) *Biochemistry 13*, 2967.
Siders, P., Cave, R. J., & Marcus, R. A. (1984) *J. Chem. Phys. 81*, 5613.
Smoluchowski, M. V. (1916) *Phys. Z. 17*, 557.
Solc, K., & Stockmayer, W. H. (1973) *Int. J. Chem. Kinet. 5*, 733.
Stonehuerner, J., Williams, J. B., & Millett, F. (1979) *Biochemistry 18*, 5422.
Strittmatter, P. (1964) in *Rapid Mixing and Sampling in Biochemistry* (Chance, B., Eisenhardt, R., Gibson, Q. H., & Lundberg-Holm, K., Eds.) p 71, Academic Press, New York.
Summers, F. E., & Erman, J. E. (1988) *J. Biol. Chem. 263*, 14267.
Takano, T., & Dickerson, R. E. (1980) *Proc. Natl. Acad. Sci. U.S.A. 77*, 6371.
Takano, T., & Dickerson, R. E. (1981) *J. Mol. Biol. 153*, 95.
Tanaka, T., Takahashi, M., & Asada, K. (1981) *Plant Cell Physiol. 22*, 33.
Tanford, C., & Kirkwood, J. G. (1957) *J. Am. Chem. Soc. 79*, 5333.
Tanford, C., & Roxby, R. (1972) *Biochemistry 11*, 2192.
van Leeuwen, J. W. (1983) *Biochim. Biophys. Acta 743*, 408.
von Bodman, S. B., Schuler, M. A., Jollie, D. R., & Sligar, S. G. (1986) *Proc. Natl. Acad. Sci. U.S.A. 83*, 9443.
Wendoloski, J. J., Matthew, J. B., Weber, P. C., & Salemme, F. R. (1987) *Science 238*, 794.
Wood, P. M. (1974) *Biochim. Biophys. Acta 357*, 370.

Topology of Subunits of the Mammalian Cytochrome *c* Oxidase: Relationship to the Assembly of the Enzyme Complex†

Yu-Zhong Zhang, Gary Ewart, and Roderick A. Capaldi*
Institute of Molecular Biology, University of Oregon, Eugene, Oregon 97405
Received November 14, 1990; Revised Manuscript Received January 17, 1991

ABSTRACT: The arrangement of three subunits of beef heart cytochrome *c* oxidase, subunits Va, VIa, and VIII, has been explored by chemical labeling and protease digestion studies. Subunit Va is an extrinsic protein located on the C side of the mitochondrial inner membrane. This subunit was found to label with *N*-(4-azido-2-nitrophenyl)-2-aminoethane[^{35}S]sulfonate and sodium methyl 4-[^{3}H]formylphenyl phosphate in reconstituted vesicles in which 90% of cytochrome *c* oxidase complexes were oriented with the C domain outermost. Subunit VIa was cleaved by trypsin both in these reconstituted vesicles and in submitochondrial particles, indicating a transmembrane orientation. The epitope for a monoclonal antibody (mAb) to subunit VIa was lost or destroyed when cleavage occurred in reconstituted vesicles. This epitope was localized to the C-terminal part of the subunit by antibody binding to a fusion protein consisting of glutathione *S*-transferase (G-ST) and the C-terminal amino acids 55–85 of subunit VIa. No antibody binding was obtained with a fusion protein containing G-ST and the N-terminal amino acids 1–55. The mAb reaction orients subunit VIa with its C-terminus in the C domain. Subunit VIII was cleaved by trypsin in submitochondrial particles but not in reconstituted vesicles. N-Terminal sequencing of the subunit VIII cleavage product from submitochondrial particles gave the same sequence as the untreated subunit, i.e., ITA, indicating that it is the C-terminus which is cleaved from the M side. Subunits Va and VIII each contain N-terminal extensions or leader sequences in the precursor polypeptides; subunit VIa is made without an N-terminal extension.

The mammalian cytochrome *c* oxidase is a multisubunit enzyme made up of 13 different subunits, each of which has been fully sequenced [e.g., see Anderson et al. (1981), Meinecke et al. (1984), and Meinecke and Buse (1985)] and for many of which the genes have been cloned and characterized [reviewed in Cao et al. (1988), Lomax and Grossman (1989),

† This work was supported by NIH Grant HL22050.

0006-2960/91/0430-3674$02.50/0